

Vibronic spectroscopy of unsaturated transition metal complexes: CrC₂H, CrCH₃, and NiCH₃

Dale J. Brugh,^{a)} Ryan S. DaBell,^{b)} and Michael D. Morse^{c)}
Department of Chemistry, University of Utah, Salt Lake City, Utah 84112

(Received 27 July 2004; accepted 29 September 2004)

Vibronically resolved resonant two-photon ionization and dispersed fluorescence spectra of the organometallic radicals CrC₂H, CrCH₃, and NiCH₃ are reported in the visible and near-infrared wavelength regions. For CrC₂H, a complicated vibronic spectrum is found in the 11 100–13 300 cm⁻¹ region, with a prominent vibrational progression having $\omega'_e = 426.52 \pm 0.84$ cm⁻¹, $\omega'_e x'_e = 0.74 \pm 0.13$ cm⁻¹. Dispersed fluorescence reveals a $v'' = 1$ level of the ground state with $\Delta G''_{1/2} = 470 \pm 20$ cm⁻¹. These vibrational frequencies undoubtedly pertain to the Cr–C₂H stretching mode. It is suggested that the spectrum corresponds to the $\tilde{A}^6\Sigma^+ \leftarrow \tilde{X}^6\Sigma^+$ band system, with the CrC₂H molecule being linear in both the ground and the excited state. The related CrCH₃ molecule displays a vibronic spectrum in the 11 500–14 000 cm⁻¹ region. The upper state of this system displays six sub-bands that are too closely spaced to be vibrational structure, but too widely separated to be *K* structure. It is suggested that the observed spectrum is a ${}^6E \leftarrow \tilde{X}^6A_1$ band system, analogous to the well-known $B^6\Pi \leftarrow X^6\Sigma^+$ band systems of CrF and CrCl. The ground state Cr–CH₃ vibration is characterized by $\omega''_e = 525 \pm 17$ cm⁻¹ and $\omega''_e x''_e = 7.9 \pm 6$ cm⁻¹. The spectrum of NiCH₃ lies in the 16 100–17 400 cm⁻¹ range and has $\omega'_e = 455.3 \pm 0.1$ cm⁻¹ and $\omega'_e x'_e = 6.60 \pm 0.03$ cm⁻¹. Dispersed fluorescence studies provide ground state vibrational constants of $\omega''_e = 565.8 \pm 1.6$ cm⁻¹ and $\omega''_e x''_e = 1.7 \pm 3.0$ cm⁻¹. Again, these values correspond to the Ni–CH₃ stretching motion. © 2004 American Institute of Physics. [DOI: 10.1063/1.1821497]

I. INTRODUCTION

One of the primary justifications for the spectroscopic investigation of small transition metal clusters and organometallic radicals is that these species serve as models for understanding aspects of catalytic processes. It is clear that understanding the fundamental properties of small transition metal systems can aid our understanding of larger catalytic systems. Even if there is no direct and immediate application to real world catalysis, the determination of precise electronic and geometric parameters for such molecules is important so that theoretical methods can be put to the test. To this end, much effort has been expended to characterize the electronic, geometric, thermodynamic, and spectroscopic parameters of small transition metal clusters.^{1–7} A similarly large effort has been made to characterize diatomic transition metal oxides, nitrides, and carbides.^{8–22}

In addition to these pure metallic clusters and diatomic molecules, a handful of more complicated polyatomic organometallic radicals involving open *d*-subshell transition metals have been investigated using gas phase spectroscopic methods. These include the transition metal methylidyne TiCH,²³ VCH,²⁴ NbCH,²⁵ TaCH,²⁶ and WCH,²⁷ the dicarbide YC₂,^{28,29} the acetylide YbCCH,³⁰ and the cyanides CuCN³¹ and NiCN.³² Spectroscopic studies of filled (or empty) *d*-subshell organometallic radicals such as MgCH₃,³³

CaCH₃,^{34–36} SrCH₃,^{34,37} BaCH₃,³⁸ ZnCH₃,^{39,40} CdCH₃,^{39,41,42} MgCCH,^{43,44} CaCCH,^{45–47} SrCCH,^{45,48} NaCH,⁴⁹ KCH,⁴⁹ and CaC₅H₅⁵⁰ have been very successful and abundant, but these molecules generally lack the connection to catalytic chemistry that is a primary motivation for the study of transition metal organometallic radicals.

To add to our knowledge of the spectroscopy and electronic structure of organometallic radicals containing open *d*-subshell transition metals, we have conducted investigations into the electronic spectroscopy of CrC₂H, CrCH₃, and NiCH₃. In this paper we report on the vibrationally resolved resonant two-photon ionization (R2PI) and dispersed fluorescence (DF) spectra of these molecules. Attempts to assign the rotationally resolved spectra are currently underway. The results of the rotationally resolved work will be reported elsewhere, if successful.

II. EXPERIMENT

All of the molecules investigated in this report were generated by pulsed laser ablation of a pure chromium or nickel disk in the throat of a supersonic expansion of helium containing 3% methane. For the R2PI studies, laser ablation of the metal target was achieved using the second harmonic radiation of a pulsed Nd:YAG (YAG—yttrium aluminum garnet) laser (532 nm); for the DF studies, the fundamental of a Nd:YAG laser (1064 nm) was used. For the production of CrC₂H and CrCH₃, the molecular signal was optimized at very low ablation laser energies— ≈ 2 mJ/pulse. Production

^{a)}Present address: Department of Chemistry, Ohio Wesleyan University, Delaware, OH.

^{b)}Present address: Department of Chemistry, Brigham Young University, Idaho, Rexburg, ID.

^{c)}Electronic mail: morse@chem.utah.edu

of NiCH₃ was also optimized at low ablation laser energies. The nozzle backing pressure was maintained close to 80 psi for all investigations.

In the R2PI studies, excitation photons were provided by the output of either a pulsed dye laser (Molelectron) or by an optical parametric oscillator/optical parametric amplifier (OPO/OPA) laser (Continuum, Mirage 500). In either case, the tunable laser was pumped by a Nd:YAG laser. The ionization photons used in the R2PI investigations were obtained from a Lambda-Physik excimer laser operating on an ArF fill (193 nm, 6.42 eV). The resulting ions were detected using a reflectron time-of-flight mass spectrometer⁵¹ equipped with a Wiley-McLaren extraction source.⁵² The time-of-flight mass spectra were digitized and stored in a PC-based computer, which was also used to control the timing of the experimental cycle. A copper box cooled to liquid nitrogen temperature via an attached dewar was used to reduce the oil vapor pressure in the ionization chamber. Use of this cold shroud was essential for this investigation because a major fragment of the diffusion pump oil (Santovac 5) is phenyl (C₆H₅), which has a mass of 77 amu; this is also the mass of ⁵²Cr¹²C₂H, one of the species investigated in this report. Without the cold shroud, the interfering signal due to phenyl could at times cause complete saturation of the detector, eliminating any hope of extracting useful information. The cold shroud reduced this background signal several orders of magnitude, so that an optical spectrum could be recorded at mass 77 without a significant background signal due to diffusion pump oil.

For dispersed fluorescence experiments, molecules in the supersonic expansion were interrogated using radiation from a pulsed dye laser (Lambda-Physik) pumped by the second harmonic of a Nd:YAG laser (Continuum). The fluorescent emission was collected at right angles to the molecular beam and the excitation laser, imaged onto the entrance slit of a 0.5 m spectrograph (F/6.5, Acton Research Corp.) and dispersed using a 300 lines/mm diffraction grating (500 nm blaze) before being imaged onto the head of an intensified charge coupled device (ICCD) array (Roper Scientific). The ICCD was gated to limit noise, and the data were read out and stored on a PC-based computer for subsequent analysis.

The emission spectra obtained from different excitations of a given molecule were placed on a common relative scale by subtracting the emission frequency from the excitation frequency, resulting in data presented in relative wave numbers, as $\nu_{\text{ex}} - \nu_{\text{em}} = \nu_{\text{rel}}$, where ν_{em} , ν_{ex} , and ν_{rel} are the emission frequency, excitation frequency, and relative frequency, respectively. The resulting values of ν_{rel} provide the energy of the ground state vibrational levels, relative to the zero-point level.

III. RESULTS

Because rather few spectroscopic investigations of open *d*-subshell polyatomic metal-ligand complexes have been reported, it seems worthwhile to first show an example of the molecules that can be produced with the laser vaporization/supersonic expansion source when methane is reacted with the ablated atoms. This provides a hint as to the potential

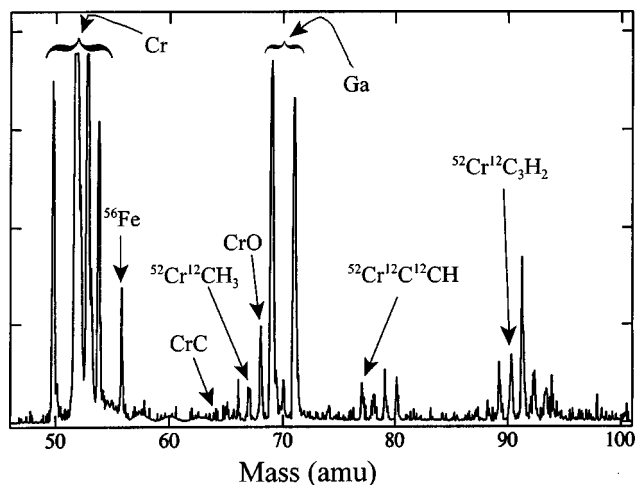


FIG. 1. Mass spectrum displaying the species produced when a chromium target is laser ablated into a helium flow containing 3% CH₄, which is subsequently subjected to ArF excimer radiation (193 nm, 6.42 eV) for multiphoton ionization. The gallium mass peaks at 69 and 71 amu are the remnants of an earlier experiment that contaminated the vaporization fixture with a small amount of gallium. This is one-photon ionized at 193 nm, making it very efficiently detected.

richness of future work in this field. Figure 1 illustrates the products formed when a pure Cr sample is ablated in the presence of methane and the molecular beam is interrogated with an ArF excimer laser. In addition to atomic Cr, Cr₂, and CrC, a number of identifiable polyatomic species are present, including CrCH_{*n*} (*n*=0–3), CrC₂H_{*n*} (*n*=1–4), and CrC₃H_{*n*} (*n*=0–5). Unlike many of the other transition metals that we have investigated, Cr readily forms a wide variety of organometallic radicals under these laser ablation conditions. Furthermore, the R2PI spectroscopic method has demonstrated that many of these chromium radicals have spectra in the near-infrared region of the spectrum. In spectral scans over the range from 10 500 to 15 500 cm⁻¹ (950 to 650 nm), R2PI spectra have been found for CrH, CrC, CrCH, CrCH₃, CrC₂H, CrC₃H₂, and CrC₃H₃. Among the polyatomic chromium organometallic radicals, the most readily interpreted spectra were found for CrC₂H and CrCH₃, so this paper concentrates on these species. Dispersed fluorescence work completed on these molecules has also provided information on the ground state; unfortunately, however, the cutoff of the ICCD detector at about 11 000 cm⁻¹ restricted the amount of information that could be obtained.

A. CrC₂H

The R2PI vibronic spectrum of CrC₂H is displayed in Fig. 2. The observed bands are listed in Table I, along with lifetimes measured by the time-delayed two-photon ionization method and the $\nu(^{52}\text{Cr}^{12}\text{C}_2\text{H}) - \nu(^{53}\text{Cr}^{12}\text{C}_2\text{H})$ isotope shift. In Table I, bands are grouped into progressions, with the most intense and obvious progressions listed as *A*, *B*, and *C*. These appear near the 0-0, 1-0, 2-0, etc., labels in Fig. 2. Members of the *A*, *B*, and *C* progressions can be fit to the standard anharmonic oscillator formula to obtain values of ($\omega'_e, \omega'_e x'_e$) in cm⁻¹ of (426.5±1.1, 0.70±0.17), (425.7±1.4, 0.65±0.23), and (431.5±3.4, 1.74±0.55), respectively. Within the error limits, these values are in good agreement,

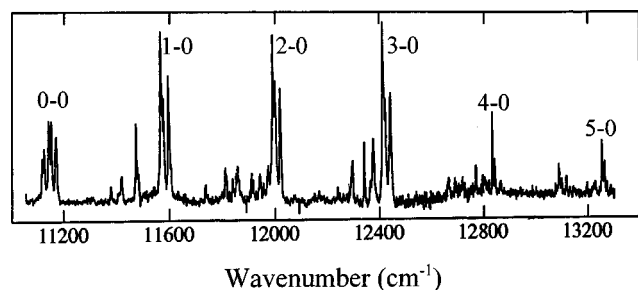


FIG. 2. Resonant two-photon ionization spectrum of $^{52}\text{CrC}_2\text{H}$, recorded using ArF excimer radiation (193 nm, 6.42 eV) to provide the ionization photon.

so taking a weighted average of these values, we assign the progression-forming normal mode values of $\omega'_e = 426.52 \pm 0.84 \text{ cm}^{-1}$, $\omega'_e x'_e = 0.74 \pm 0.13 \text{ cm}^{-1}$.

This vibrational mode is almost certainly the metal-carbon stretch, because the electronic excitation is centered on the chromium atom, so that the metal-carbon bonding is disturbed in the excitation. Thus, a significant progression in the metal-carbon stretching mode is expected. In addition, this vibrational frequency is similar to that found in other systems having a single metal-carbon bond. For example, the ground states of the $3d$ monomethyl molecules are calculated to have vibrational frequencies in the range of 465–569 cm^{-1} .⁵³

Dispersed fluorescence studies on CrC_2H were difficult because of the long lifetime of the upper state and the lack of sensitivity of the detector in the near infrared region. Nevertheless, fluorescence was observed to the $v'' = 1$ level when bands in the 2-0 and 3-0 groups of transitions were excited. These results provide $\Delta G''_{1/2} = 470 \pm 20 \text{ cm}^{-1}$, where the large error limit results from the poor intensity of the $v'' = 1$ feature in the spectrum. This vibrational interval corresponds to the ground state Cr–C stretching vibration, which drops in frequency by about 45 cm^{-1} upon electronic excitation. The drop in vibrational frequency suggests that the Cr–C bond lengthens when the molecule is electronically excited, a possibility that is certainly consistent with the long vibrational progression that is observed.

The vibronic spectrum displayed in Fig. 2 is rather more complicated than one might expect for a molecule with so few vibrational degrees of freedom. Some of these features may be due to vibrational hot bands, but we find no additional features to the red of what is displayed in Fig. 2. Alternatively, mixing with underlying dark states may lead to the large number of vibronic transitions observed. This latter possibility could explain the variation in excited state lifetimes that is observed, with measured values ranging from 1.06 ± 0.10 to $2.13 \pm 0.40 \mu\text{s}$. It is likely that some of the less intense, unmeasured features observed in the spectrum could have even longer lifetimes.

B. CrCH_3

The vibronic spectrum of CrCH_3 was recorded using R2PI spectroscopy and is displayed in Fig. 3. This figure juxtaposes two spectra that were collected under different

TABLE I. CrC_2H band positions, lifetimes, and isotope shifts.

Progression	v''^a	Wave number ^b (cm^{-1})	Lifetime (μs)	Isotope ^c shift (cm^{-1})
		11 120.1		
		11 126.7		
A	0	11 143.9(−0.4)	1.09(33)	0.6
A	1	11 570.1(0.8)	1.53(10)	2.4
A	2	11 992.3(−0.7)	1.64(36)	3.6
A	3	12 416.1(0.9)	1.50(14)	4.7
A	4	12 835.0(−1.1)		5.5
A	5	13 256.0(0.5)		
B	0	11 154.3(−0.7)	1.29(35)	0.6
B	1	11 580.8(1.4)	1.47(39)	2.4
B	2	12 001.9(−0.7)	1.94(42)	1.7
B	3	12 425.1(0.7)	1.76(29)	
B	4	12 843.5(−1.4)		
B	5	13 264.9(0.7)		
C	0	11 171.9(0.3)	1.06(10)	0.9
C	1	11 600.9(1.3)	1.37(22)	1.5
C	2	12 020.7(−3.5)	1.44(30)	3.3
C	3	12 445.2(0.0)	2.13(40)	
C	4	12 866.8(4.0)		
C	5	13 274.9(−2.0)		
D	0	11 380.3(−0.1)		
D	1	11 812.5(−0.3)		
D	2	12 243.1(1.0)		
D	4	13 090.5(−1.1)		
D	5	13 512.5(0.6)		
E	0	11 420.2 ^d		
E	1	11 837.7 ^d		
E	2	12 271.7 ^d		
F	0	11 476.0(0.1)		
F	1	11 909.7(−0.6)		
F	2	12 343.1(0.9)		
F	3	12 770.8(−0.6)		
F	4	13 198.2(0.2)		
G	1	11 942.8 ^d		
G	2	12 366.5 ^d		
G	3	12 796.9 ^d		
Unassigned		11 736.5		
Unassigned		11 856.7		
Unassigned		11 974.2		
Unassigned		12 295.3		
Unassigned		12 378.0		
Unassigned		13 100.3		
Fitted vibronic parameters				
Progression	T_0	ω'_e	$\omega'_e x'_e$	
A	11 144.26(0.96)	426.46(1.07)	0.70(0.17)	
B	11 155.00(1.27)	425.73(1.42)	0.65(0.23)	
C	11 171.61(3.06)	431.51(3.41)	1.74(0.55)	
D	11 380.43(1.06)	435.40(1.34)	1.52(0.22)	
E ^d	11 420.22 ^d	400.80 ^d	−8.32 ^d	
F	11 475.84(0.84)	437.06(1.23)	1.30(0.24)	
G ^d	11 525.63 ^d	410.56 ^d	−3.30 ^d	

^aThese quantum numbers denote the number of quanta of the Cr–C₂H stretching vibration present in the upper electronic states.

^bThe band positions were measured from low resolution survey scans for the $^{52}\text{Cr}^{12}\text{C}_2\text{H}$ isotope and are believed to have an uncertainty of 0.5 cm^{-1} . Residuals in the vibronic fits are given in parentheses following each measured band position.

^cThe isotope shift is reported as the value of $\nu(^{52}\text{Cr}^{12}\text{C}_2\text{H}) - \nu(^{53}\text{Cr}^{12}\text{C}_2\text{H})$. These values were measured from low resolution survey scans and are also believed to be accurate to 0.5 cm^{-1} . Where values are not reported, the vibronic feature was unobserved in the spectrum of $^{53}\text{Cr}^{12}\text{C}_2\text{H}$.

^dFor the E and G progressions, only three bands were found, so T_0 , ω'_e , and $\omega'_e x'_e$ are uniquely determined and their errors cannot be estimated.

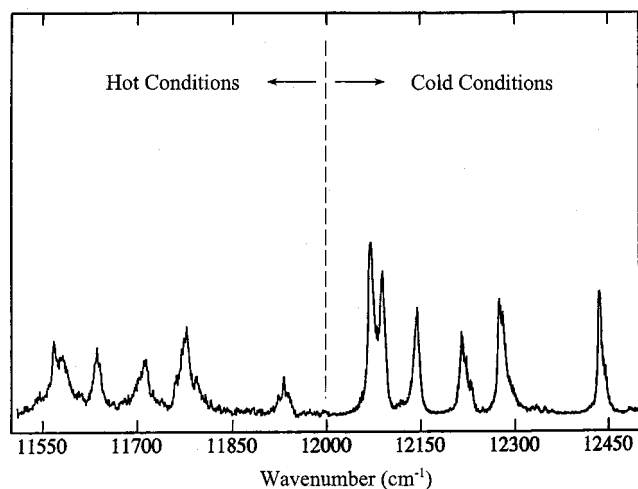


FIG. 3. Resonant two-photon ionization spectrum of $^{52}\text{CrCH}_3$, recorded using ArF excimer radiation (193 nm, 6.42 eV) to provide the ionization photon. To the red of $12\,000\text{ cm}^{-1}$ the spectrum was collected using 80 psi backing pressure and a 2 mm expansion orifice. To the blue of $12\,000\text{ cm}^{-1}$, a backing pressure of 120 psi and a 1 mm expansion orifice were employed, providing colder conditions. The bands to the red of $12\,000\text{ cm}^{-1}$ were not observed under these colder conditions.

source conditions. To the red of $12\,000\text{ cm}^{-1}$, the spectrum was collected using 80 psi backing pressure and a 2 mm expansion orifice. This region is labeled in the figure as having been collected under hot conditions. To the blue of $12\,000\text{ cm}^{-1}$, colder conditions were employed, in which the nozzle pressure was increased to 120 psi and the expansion orifice was narrowed to 1 mm. This latter modification effectively moved the probe region a greater number of nozzle diameters downstream, thereby cooling the molecules more effectively. All of the features to the red of $12\,000\text{ cm}^{-1}$ vanished when cold conditions were employed, establishing that they originate from thermally populated states. It is obvious in Fig. 3 that the six vibronic features observed to the red of $12\,000\text{ cm}^{-1}$ mimic the six vibronic features observed to the blue of $12\,000\text{ cm}^{-1}$, with the poorer resolution of the hot bands resulting from the greater rotational temperature obtained when the spectrum was collected under hot conditions. No transitions were observed to the red of $11\,550\text{ cm}^{-1}$ under any conditions. To the blue of $12\,500\text{ cm}^{-1}$, the spectrum becomes more congested and less amenable to interpretation. As one moves even further to the blue, the congested spectrum gradually weakens in intensity, so that very little absorption occurs beyond $14\,000\text{ cm}^{-1}$.

It is apparent in Fig. 3 that the hot bands appearing to the red of $12\,000\text{ cm}^{-1}$ are an echo of the cold bands appearing to the blue of $12\,000\text{ cm}^{-1}$. Wave numbers of both the hot and cold bands are listed in Table II, along with upper state lifetimes of the cold bands, and the frequency differences between the corresponding hot and cold bands. The agreement between these frequency differences is very good, given the breadth of the features. It is obvious that all of the hot bands originate from the same thermally populated vibrational level of the CrCH_3 ground state, and that this level lies $509.2 \pm 1.4\text{ cm}^{-1}$ above the ground vibrational level, using 1σ error limits based on the standard deviation of the mean. This value of $\Delta G''_{1/2}$ matches well with the values of ω''_e

TABLE II. Band positions of CrCH_3 .

Cold conditions		Hot conditions	
Wave number (cm^{-1})	τ (μs)	Wave number (cm^{-1})	$\Delta G''_{1/2}$ (cm^{-1})
12 072.5	2.21(10)	11 568.5	506.8 ± 1
12 089.0	2.08(10)	11 580.7	511.1 ± 1
12 142.8	1.40(10)	11 636.4	509.2 ± 1
12 219.8	3.10(10)	11 707.3	515.2 ± 1
12 279.2	3.90(20)	11 774.8	507.2 ± 1
12 435.6	2.50(10)	11 932.4	505.7 ± 1

$= 525 \pm 17\text{ cm}^{-1}$ and $\omega''_e x''_e = 7.9 \pm 6\text{ cm}^{-1}$ that were obtained in our dispersed fluorescence studies of CrCH_3 . Both values are also in good agreement with the vibrational frequency calculated for the Cr-CH₃ stretching motion in the $\text{CrCH}_3 \tilde{X}^6A_1(C_{3v})$ ground state, 537 cm^{-1} .⁵³

The rovibronic spectrum of CrCH_3 is quite complex and has not been analyzed as of yet. Given that CrCH_3 is expected to be a C_{3v} symmetric top with a 6A_1 ground state, it is not surprising that the rotationally resolved spectra are complicated. In fact, to our knowledge no rotationally resolved optical spectrum of a nonlinear sextet molecule has ever been analyzed. The appropriate Hamiltonian will have to be developed in order to analyze this spectrum.

C. NiCH₃

We have recently recorded and published the optical spectrum of diatomic NiC.¹¹ During our investigation of NiC, spectroscopic transitions were observed in NiCH_3 as well. The vibronic spectrum, recorded using R2PI spectroscopy and displayed in Fig. 4, displays three intense features along with transitions of lesser intensity. Four of the observed bands can be assigned to a progression with $\omega'_e = 455.3 \pm 0.1\text{ cm}^{-1}$ and $\omega'_e x'_e = 6.58 \pm 0.03\text{ cm}^{-1}$ for $^{58}\text{NiCH}_3$. Without a doubt, this frequency corresponds to a progression in the Ni-CH₃ stretching mode, since electronic excitations localized on the CH₃ group are expected to occur at much shorter wavelengths. In addition to the R2PI work, DF spectra have been collected for this molecule. Figure 5

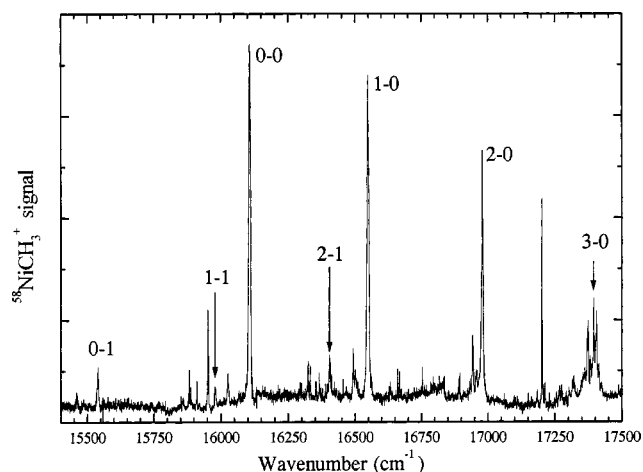


FIG. 4. Resonant two-photon ionization spectrum of $^{58}\text{NiCH}_3$, recorded using ArF excimer radiation (193 nm, 6.42 eV) to provide the ionization photon.

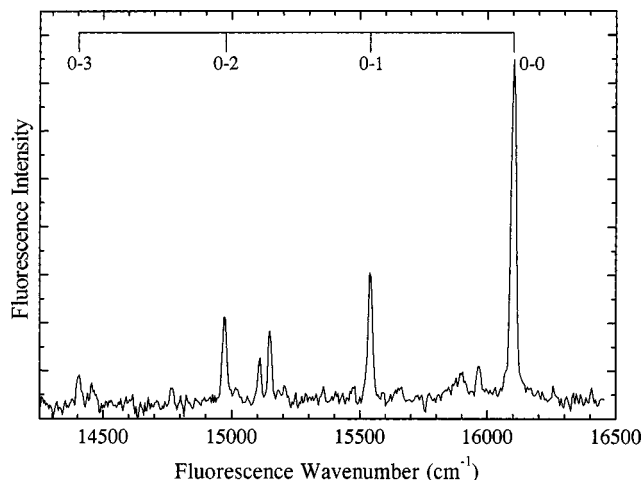


FIG. 5. Dispersed fluorescence obtained following the irradiation of a molecular beam containing NiCH₃ at the frequency of the 16 107 cm⁻¹ 0-0 band of Fig. 4.

displays the fluorescence that results when the 0-0 band at 16 107 cm⁻¹ is excited. Dispersed fluorescence collected from the excitation of these bands yields values of $\omega_e'' = 565.8 \pm 1.6$ cm⁻¹ and $\omega_e''x_e'' = 1.7 \pm 3.0$ cm⁻¹. Again, this progression undoubtedly corresponds to the Ni-CH₃ stretching mode. This ground state vibrational frequency compares very well to the calculated Ni-CH₃ vibrational frequency of 555 cm⁻¹.⁵³ The excited state lifetimes of the bands in this progression are all very long, near 10 μ s, but they are consistent, lending support to their grouping into a progression. The positions of the bands for both the ⁵⁸Ni¹²CH₃ and ⁶⁰Ni¹²CH₃ isotopes and their upper state lifetimes, as measured from low resolution survey scans, are listed in Table III.

We have attempted to rotationally resolve the 0-0, 1-0, and 2-0 bands that are displayed in Fig. 4. The spectra are dominated by surprisingly few lines, and vary quite a bit from band to band and between the ⁵⁸NiCH₃ and ⁶⁰NiCH₃ isotopomers. The variability of these features, particularly between the ⁵⁸NiCH₃ and ⁶⁰NiCH₃ isotopomers, indicates

TABLE III. Band positions of NiCH₃. Fitted vibrational constants for ⁵⁸NiCH₃: $T_0 = 16\,107.42 \pm 0.07$ cm⁻¹; $\omega_e' = 455.29 \pm 0.14$ cm⁻¹; $\omega_e'x_e' = 6.57 \pm 0.03$ cm⁻¹. Residuals in the fit of the ⁵⁸NiCH₃ bands are reported in parentheses next to the measured band positions. For ⁶⁰NiCH₃, no error limits could be estimated because only three bands were found. For these three bands a unique vibronic fit was obtained, giving $T_0 = 16\,108.3$ cm⁻¹; $\omega_e' = 450.9$ cm⁻¹; $\omega_e'x_e' = 5.65$ cm⁻¹. Because of the weak intensity of the hot bands, which were only identified after the dispersed fluorescence work had been completed, these features were not included in the fit.

$v'-v''$	$\nu(^{58}\text{NiCH}_3)$ (cm ⁻¹)	$\nu(^{60}\text{NiCH}_3)$ (cm ⁻¹)	τ (μ s)	Isotope shift ^a (cm ⁻¹)
0-0	16 107.4(0.0)	16 108.3	9.6 \pm 0.1	0.9
1-0	16 549.6(0.1)	16 547.9	11.1 \pm 0.3	-1.7
2-0	16 978.5(-0.1)	16 976.2	11.6 \pm 0.4	-2.3
3-0	17 394.4(0.0)
0-1	15 539.9	15 542.6		2.7
1-1	15 978.7	15 979.2		0.5
2-1	16 404.4	16 403.7		-0.7

^aThe isotope shift is reported as $\nu(^{60}\text{NiCH}_3) - \nu(^{58}\text{NiCH}_3)$.

that these levels are likely perturbed by other nearby vibronic states. The rotationally resolved spectra have thus far eluded analysis, although we remain hopeful that additional efforts will permit us to understand them.

No low-lying excited states of NiCH₃ could be identified with certainty in the dispersed fluorescence, although a manifold of low-lying electronic states arises from the 3d⁹, ²D core of the nickel atom, which splits into a ²A₁ and two ²E terms in the C_{3v} point group. The ²E terms are split further into E_{1/2} and E_{3/2} terms when spin-orbit interaction is considered. Two weak features in the DF spectrum displayed in Fig. 5, lying at 15 148 and 15 111 cm⁻¹ (which correspond to energies of 956 and 993 cm⁻¹ above the ground level) are obviously not part of the progression in the Ni-CH₃ stretching mode. These features could correspond to vibrational levels within the NiCH₃ ground electronic state or to vibrational levels of other states. *Ab initio* calculations⁵⁴ and IR studies⁵⁵ of the related molecule, CuCH₃, show that this molecule has no vibrational motions with frequencies between 670 and 1140 cm⁻¹. Because NiCH₃ is expected to be similar to CuCH₃ in its vibrational frequencies, it seems unlikely that these features between 950 and 1000 cm⁻¹ could be due to fluorescence to excited vibrational levels of the ground state. The presence of a Jahn-Teller effect in the ²E ground state could complicate the vibronic structure, but the large spin-orbit splitting expected for NiCH₃ (the splitting in NiH is about 1000 cm⁻¹) (Ref. 56) will largely quench this effect. Fluorescence to the other low-lying excited states arising from the 3d⁹, ²D core of the nickel atom is a likely explanation of these features. We have not been able to definitively confirm this tantalizing possibility as of yet. Alternatively, these features may correspond to emissions from an impurity species in the beam. Fluorescence from impurities in the molecular beam dominated the fluorescence when the 1-0 absorption band was excited near 16 550 cm⁻¹, so that no useful information could be obtained.

IV. DISCUSSION

Even though rotational analyses are not yet complete, comparisons to theoretical results, and to analogous isovalent molecules, have allowed us to make progress in understanding the spectra of these species.

A. CrC₂H

Though no theoretical calculations exist for CrC₂H, the fact that the vibrational frequency of the excited state is lower than that of the ground state suggests that the bond length of the excited state is longer than that of the ground state. This conclusion is supported by a comparison with isovalent CrF, where a decrease in ω_e from ground to excited state is also accompanied by a concomitant increase in the bond length.⁵⁷ Further progress in understanding CrC₂H may be obtained by other comparisons to CrF. The ground state of CrF is known to be of ⁶ Σ^+ symmetry. The bond in this molecule is essentially a σ bond derived from the spin pairing of the lone electron on F(2s²2p⁵, ²P^o) with the 4s electron on Cr(3d⁵4s¹, ²S). This leaves the 3d⁵, ⁶S core of the Cr atom intact, generating a multiplicity of 6 for the Σ^+ ground state. The electron affinity of atomic fluorine is 3.399

± 0.003 eV,⁵⁸ suggesting that it is best to think of CrF as an ionic molecule, Cr^+F^- . It is also known that the ground state of the C_2H radical is ${}^2\Sigma^+$ in symmetry⁵⁹ and that its electron affinity is 2.969 ± 0.006 eV.⁶⁰ The value of the electron affinity is similar to that of atomic fluorine, suggesting that the bonding of C_2H to Cr might be expected to be similar to that of F to Cr. Based on this comparison, the ground state of CrC_2H would be expected to be linear and of ${}^6\Sigma^+$ symmetry. It would also be expected to be very polar or even ionic, based on the large electron affinity of C_2H .

There is an additional feature of the low resolution spectrum that suggests the ground state is ${}^6\Sigma^+$ in symmetry. As listed in Table I, each of the most intense features is split into three sub-bands with spacings of roughly 10 and 18 cm^{-1} . This sub-band splitting is suggestive of the expected zero-field splitting of a ${}^6\Sigma^+$ state into its $\Omega=1/2$, $3/2$, and $5/2$ components in the Hund's case (a) limit. In terms of the zero-field splitting parameter, D , these components are expected to have a separation of $2D$ between the $\Omega=1/2$ and $\Omega=3/2$ levels and a separation of $4D$ between the $\Omega=3/2$ and $\Omega=5/2$ levels.⁶¹ In terms of the effective spin-spin interaction parameter, λ , the splittings are 4λ and 8λ , respectively.⁶² If both the upper and lower states were Hund's case (a) ${}^6\Sigma^+$ states, it might be expected that the rotationally resolved spectra of the three sub-bands could be fit as $1/2 \leftarrow 1/2$, $3/2 \leftarrow 3/2$, and $5/2 \leftarrow 5/2$ transitions, in terms of Ω , and the three sub-bands would have separations of $4(\lambda' - \lambda'')$ and $8(\lambda' - \lambda'')$, respectively. Based on the measured splittings, this would imply that $(\lambda' - \lambda'') \approx 2.4\text{ cm}^{-1}$. The rotationally resolved spectra are much more complicated than what would be expected for a ${}^6\Sigma^+(a) \leftarrow {}^6\Sigma^+(a)$ transition, however, and we have thus far been unsuccessful in our attempts at analysis. If one of the states were more appropriately described as belonging to Hund's case (b), however, many additional branches would be observed and a more complicated structure would be expected. Because the ground state is probably well isolated from nearby states, it seems likely that it belongs to case (b) while the excited state may belong to Hund's case (a). If so, the splitting of each band into three sub-bands would largely be the result of the spin-spin splitting in the excited ${}^6\Sigma^+$ state. This would be a result of off-diagonal spin-orbit interactions between the ${}^6\Sigma^+$ state and other electronic states. Based on these considerations, the observed band structure suggests that we are observing the $\tilde{A} {}^6\Sigma^+ \leftarrow \tilde{X} {}^6\Sigma^+$ transition of the linear CrCCH molecule. This hypothesis may be confirmed or rejected only by a successful rotational analysis or an accurate *ab initio* calculation.

B. CrCH_3

The ground state of CrCH_3 is expected to arise from the combination of a ground state ($3d^5 4s^1, {}^7S$) Cr atom with the methyl radical, which has a planar ${}^2A_2''$ ground state in the D_{3h} point group, with a single unpaired electron in a $p\pi$ orbital that is perpendicular to the plane of the molecule.⁵³ Spin pairing of the $4s$ electron of Cr and the unpaired $p\pi$ electron of the methyl radical results in a $\text{Cr}-\text{CH}_3\sigma^2$ bond. The Cr $3d$ electrons are left in their high spin configuration,

leaving a $3d^5, {}^6S$ core on chromium that is largely uninvolved in the bonding.⁵³ Thus, the ground state of CrCH_3 is calculated to be of 6A_1 symmetry in the C_{3v} point group.⁵³ The sequence of six strong absorptions in the R2PI absorption spectrum between 12000 cm^{-1} and 12500 cm^{-1} suggests that the upper state is also a sextet ($S=5/2$) state. It also suggests that the upper state possess residual orbital angular momentum that leads to a spin-orbit splitting of the zero-point level into six components. The preliminary conclusion, in the absence of a definitive rotational analysis, is that the transitions observed to the blue of 12000 cm^{-1} are the sub-bands of the origin band of a ${}^6E \leftarrow \tilde{X} {}^6A_1$ transition. This is analogous to the $B {}^6\Pi \leftarrow X {}^6\Sigma^+$ transitions of CrF and CrCl, located near 8134 and 8870 cm^{-1} , respectively.^{57,63}

C. NiCH_3

The ground state of NiCH_3 is calculated to be 2E in the C_{3v} point group.⁵³ This may be understood as arising from the interaction of a $3d^9 4s^1, {}^3D$ nickel atom with the ${}^2A_2''$ methyl radical. Following formation of a σ^2 bond between the $4s$ orbital of nickel and the $2p\pi$ orbital of the methyl radical, one is left with a $3d_{\text{Ni}}^9\sigma^2$ configuration, exactly as in the analogous NiH molecule. In a diatomic such as NiH, the $3d_{\text{Ni}}^9\sigma^2$ configuration leads to Hund's case (a) basis states of ${}^2\Sigma^+$, ${}^2\Pi_{1/2}$, ${}^2\Pi_{3/2}$, ${}^2\Delta_{3/2}$, and ${}^2\Delta_{5/2}$. The ground state of NiH is now known to be ${}^2\Delta_{5/2}$, and there is extensive spin-orbit mixing between the higher energy ${}^2\Sigma^+$ and ${}^2\Pi_{1/2}$ states and between the ${}^2\Pi_{3/2}$ and ${}^2\Delta_{3/2}$ states.⁵⁶ All five of these states lie within 5000 cm^{-1} of the ground state,⁵⁶ and it is expected that a similar manifold of five states arising from a $3d_{\text{Ni}}^9\sigma^2$ configuration will be present in NiCH_3 . The 2E state calculated to be the ground state of NiCH_3 derives from a $d\sigma^2 d\pi^4 d\delta^3\sigma^2$ configuration analogous to the NiH ${}^2\Delta$ ground state. In the C_{3v} double group that is applicable to NiCH_3 , the 2E state is expected to resolve into $E_{1/2}$ and $E_{3/2}$ states, with $E_{1/2}$ emerging as the ground state because of its correlation to ${}^2\Delta_{5/2}$.⁶⁴

The optical spectra of NiH have been investigated in detail,⁶⁵⁻⁶⁷ and it is now quite clear that upper states in the $15000-18000\text{ cm}^{-1}$ range correlate to $\text{Ni } 3d^8 4s^2, {}^3F + \text{H } 1s^1, {}^2S$. A large number of states (${}^2\Sigma^-, {}^2\Pi, {}^2\Delta, {}^2\Phi, {}^4\Sigma^-, {}^4\Pi, {}^4\Delta, \text{ and } {}^4\Phi$) arise from this limit. These upper states may be described in molecular terms as $3d_{\text{Ni}}^8({}^3F)\sigma^2\sigma^*$ states, and it is likely that this designation may be equally well applied to the excited state of NiCH_3 observed in the $16000-17400\text{ cm}^{-1}$ range. The excited state lifetime of about $10\text{ }\mu\text{s}$ is comparable to the upper state lifetimes of doublet states arising from the analogous $3d_{\text{Ni}}^8({}^3F)3d_{\text{Cu}}^{10}\sigma^2\sigma^*$ configuration of NiCu, which were found to have lifetimes in the range of $5-10\text{ }\mu\text{s}$.³⁷ In contrast, quartet states arising from the $3d_{\text{Ni}}^8({}^3F)3d_{\text{Cu}}^{10}\sigma^2\sigma^*$ configuration of NiCu were found to have lifetimes in excess of $40\text{ }\mu\text{s}$. This suggests that the upper state of the observed band system of NiCH_3 is primarily doublet in character. In view of the strong spin-orbit interactions among the $3d_{\text{Ni}}^8({}^3F)\sigma^2\sigma^*$ states, it is likely that the electron spin will be strongly coupled to the C_3 axis in the upper state as well as

in the ground state. Both states are expected to be well described in terms of Hund's case (a) or case (c) basis functions, leading to a classification of the observed band system as either $E_{1/2} \leftarrow E_{1/2}$ or $E_{3/2} \leftarrow E_{1/2}$ in the C_{3v} double group.

V. CONCLUSION

Studies of the electronic spectra of open d -subshell organometallic radicals are still rare in the spectroscopic literature. In this paper we have presented the first electronic spectra of three such species: CrC_2H , CrCH_3 , and NiCH_3 . Although definitive assignments will have to await the successful analysis of rotationally resolved spectra, it is suggested that the observed spectra correspond to the $\tilde{A}^6\Sigma^+ \leftarrow \tilde{X}^6\Sigma^+$ band system of linear CrC_2H , a ${}^6E \leftarrow \tilde{X}^6A_1$ band system of CrCH_3 (C_{3v} geometry), and a $3d_{\text{Ni}}^8({}^3F)\sigma^2\sigma^*(S = 1/2) \leftarrow \tilde{X}^2E(E_{1/2})$ system in NiCH_3 (C_{3v} geometry). Metal-carbon stretching frequencies have been measured in the ground state for all three molecules, and in the excited state for CrC_2H and NiCH_3 .

ACKNOWLEDGMENTS

The authors thank the U.S. Department of Energy (Grant No. DE-FG03-01ER15176) for support of this research. The authors also thank Professor Edward M. Eyring for the use of a Lambda Physik FL2002 dye laser in the dispersed fluorescence experiments.

- ¹J. R. Lombardi and B. Davis, *Chem. Rev. (Washington, D.C.)* **102**, 2431 (2002).
- ²K. M. Ervin, *Int. Rev. Phys. Chem.* **20**, 127 (2001).
- ³P. B. Armentrout, *Annu. Rev. Phys. Chem.* **52**, 423 (2001).
- ⁴M. B. Niekelbein, *Annu. Rev. Phys. Chem.* **50**, 79 (1999).
- ⁵M. F. Jarrold, *Springer Ser. Chem. Phys.* **52**, 315 (1994).
- ⁶S. J. Riley, *Ber. Bunsenges. Phys. Chem.* **96**, 1104 (1992).
- ⁷M. D. Morse, *Chem. Rev. (Washington, D.C.)* **86**, 1049 (1986).
- ⁸T. C. Steimle, W. L. Virgo, and J. M. Brown, *J. Chem. Phys.* **118**, 2620 (2003).
- ⁹T. C. Steimle, W. L. Virgo, and D. A. Hostutler, *J. Chem. Phys.* **117**, 1511 (2002).
- ¹⁰S. M. Sicking, A. W. Smith, and M. D. Morse, *J. Chem. Phys.* **116**, 993 (2002).
- ¹¹D. J. Brugh and M. D. Morse, *J. Chem. Phys.* **117**, 10703 (2002).
- ¹²R. S. Ram, P. F. Bernath, and S. P. Davis, *J. Mol. Spectrosc.* **215**, 163 (2002).
- ¹³R. S. Ram, P. F. Bernath, S. P. Davis, and A. J. Merer, *J. Mol. Spectrosc.* **211**, 279 (2002).
- ¹⁴R. S. Ram, J. Lievin, G. Li, T. Hirao, and P. F. Bernath, *Chem. Phys. Lett.* **343**, 437 (2001).
- ¹⁵M. Fujitake, A. Toba, M. Mori, F. Miyazawa, N. Ohashi, K. Aiuchi, and K. Shibuya, *J. Mol. Spectrosc.* **208**, 253 (2001).
- ¹⁶J. F. Harrison, *Chem. Rev. (Washington, D.C.)* **100**, 679 (2000).
- ¹⁷T. C. Steimle, J. S. Robinson, and D. Goodridge, *J. Chem. Phys.* **110**, 881 (1999).
- ¹⁸J. D. Langenberg, L. Shao, and M. D. Morse, *J. Chem. Phys.* **111**, 4077 (1999).
- ¹⁹J. D. Langenberg, R. S. DaBell, L. Shao, D. Dreessen, and M. D. Morse, *J. Chem. Phys.* **109**, 7863 (1998).
- ²⁰B. Simard, P. I. Presnka, H. P. Loock, A. Bércecs, and O. Launila, *J. Chem. Phys.* **107**, 307 (1997).
- ²¹B. Simard, P. A. Hackett, and W. J. Balfour, *Chem. Phys. Lett.* **230**, 103 (1994).
- ²²A. J. Merer, *Annu. Rev. Phys. Chem.* **40**, 407 (1989).
- ²³M. Barnes, A. J. Merer, and G. F. Metha, *J. Mol. Spectrosc.* **181**, 168 (1997).
- ²⁴M. Barnes, P. G. Hajigeorgiou, R. Kasrai, A. J. Merer, and G. F. Metha, *J. Am. Chem. Soc.* **117**, 2096 (1995).
- ²⁵M. Barnes, D. A. Gillett, A. J. Merer, and G. F. Metha, in the Proceedings of 51st Ohio State International Symposium on Molecular Spectroscopy, 1996.
- ²⁶M. Barnes, D. A. Gillett, G. F. Metha, K. Athanassenas, and A. J. Merer, in the Proceedings of 51st Ohio State International Symposium on Molecular Spectroscopy, 1996.
- ²⁷M. Barnes, D. A. Gillett, A. J. Merer, and G. F. Metha, *J. Chem. Phys.* **105**, 6168 (1996).
- ²⁸R. R. Bousquet and T. C. Steimle, *J. Chem. Phys.* **114**, 1306 (2001).
- ²⁹T. C. Steimle, R. R. Bousquet, K. C. Namiki, and A. J. Merer, *J. Mol. Spectrosc.* **215**, 10 (2002).
- ³⁰H.-P. Loock, A. Bércecs, B. Simard, and C. Linton, *J. Chem. Phys.* **107**, 2720 (1997).
- ³¹D. B. Grotjahn, M. A. Brewster, and L. M. Ziurys, *J. Am. Chem. Soc.* **124**, 5895 (2002).
- ³²P. M. Sheridan and L. M. Ziurys, *J. Chem. Phys.* **118**, 6370 (2003).
- ³³M. A. Anderson and L. M. Ziurys, *Astrophys. J. Lett.* **452**, L157 (1995).
- ³⁴C. R. Brazier and P. F. Bernath, *J. Chem. Phys.* **86**, 5918 (1987).
- ³⁵C. R. Brazier and P. F. Bernath, *J. Chem. Phys.* **91**, 4548 (1989).
- ³⁶M. A. Anderson and L. M. Ziurys, *Astrophys. J. Lett.* **460**, L77 (1996).
- ³⁷M. A. Anderson, J. S. Robinson, and L. M. Ziurys, *Chem. Phys. Lett.* **257**, 471 (1996).
- ³⁸J. Xin, J. S. Robinson, A. J. Apponi, and L. M. Ziurys, *J. Chem. Phys.* **108**, 2703 (1998).
- ³⁹T. M. Cerny, X. Q. Tan, J. M. Williamson, E. S. J. Robles, A. M. Ellis, and T. A. Miller, *J. Chem. Phys.* **99**, 9376 (1993).
- ⁴⁰I. M. Povey, A. J. Bezant, G. K. Corlett, and A. M. Ellis, *J. Phys. Chem.* **98**, 10427 (1994).
- ⁴¹X. Q. Tan, T. M. Cerny, J. M. Williamson, and T. A. Miller, *J. Chem. Phys.* **101**, 6396 (1994).
- ⁴²S. I. Panov, D. E. Powers, and T. A. Miller, *J. Chem. Phys.* **108**, 1335 (1998).
- ⁴³M. A. Anderson and L. M. Ziurys, *Astrophys. J. Lett.* **439**, L25 (1995).
- ⁴⁴M. A. Brewster, A. J. Apponi, J. Xin, and L. M. Ziurys, *Chem. Phys. Lett.* **310**, 411 (1999).
- ⁴⁵A. M. R. P. Bopeggedera, C. R. Brazier, and P. F. Bernath, *Chem. Phys. Lett.* **136**, 97 (1987).
- ⁴⁶A. M. R. P. Bopeggedera, C. R. Brazier, and P. F. Bernath, *J. Mol. Spectrosc.* **129**, 268 (1988).
- ⁴⁷M. A. Anderson and L. M. Ziurys, *Astrophys. J. Lett.* **444**, L57 (1995).
- ⁴⁸B. P. Nuccio, A. J. Apponi, and L. M. Ziurys, *Chem. Phys. Lett.* **247**, 283 (1995).
- ⁴⁹J. Xin and L. M. Ziurys, *J. Chem. Phys.* **110**, 3360 (1999).
- ⁵⁰L. C. O'Brien and P. F. Bernath, *J. Am. Chem. Soc.* **108**, 5017 (1986).
- ⁵¹B. A. Mamyurin, V. I. Karataev, D. V. Shmikk, and V. A. Zagulin, *Zh. Eksp. Teor. Fiz.* **64**, 82 (1973).
- ⁵²W. C. Wiley and I. H. McLaren, *Rev. Sci. Instrum.* **26**, 1150 (1955).
- ⁵³C. W. Bauschlicher, Jr., S. R. Langhoff, H. Partridge, and L. A. Barnes, *J. Chem. Phys.* **91**, 2399 (1989).
- ⁵⁴M. Sodupe, C. W. Bauschlicher, Jr., and T. J. Lee, *Chem. Phys. Lett.* **189**, 266 (1992).
- ⁵⁵J. M. Parnis, S. A. Mitchell, J. Garcia-Prieto, and G. A. Ozin, *J. Am. Chem. Soc.* **107**, 8169 (1985).
- ⁵⁶S. Wallin, R. Koivisto, and O. Launila, *J. Chem. Phys.* **105**, 388 (1996).
- ⁵⁷H. Hotop and W. C. Lineberger, *J. Phys. Chem. Ref. Data* **14**, 731 (1985).
- ⁵⁸P. G. Carrick, A. J. Merer, and R. F. Curl, Jr., *J. Chem. Phys.* **78**, 3652 (1983).
- ⁵⁹K. M. Ervin and W. C. Lineberger, *J. Phys. Chem.* **95**, 1167 (1991).
- ⁶⁰W. Weltner, Jr., *Magnetic Atoms and Molecules* (Dover, New York, 1983).
- ⁶¹R. M. Gordon and A. J. Merer, *Can. J. Phys.* **58**, 642 (1980).
- ⁶²R. Koivisto, O. Launila, B. Schimmelpfennig, B. Simard, and U. Wahlgren, *J. Chem. Phys.* **114**, 8855 (2001).
- ⁶³J. A. Gray, M. Li, T. Nelis, and R. W. Field, *J. Chem. Phys.* **95**, 7164 (1991).
- ⁶⁴G. Herzberg, *Molecular Spectra and Molecular Structure III. Electronic Spectra and Electronic Structure of Polyatomic Molecules* (Van Nostrand Reinhold, New York, 1966).
- ⁶⁵R. Scullman, S. Lofgren, and S. A. Kadavathu, *Phys. Scr.* **25**, 295 (1982).
- ⁶⁶S. A. Kadavathu, R. Scullman, J. A. Gray, M. Li, and R. W. Field, *J. Mol. Spectrosc.* **140**, 126 (1990).
- ⁶⁷S. A. Kadavathu, R. Scullman, R. W. Field, J. A. Gray, and M. Li, *J. Mol. Spectrosc.* **147**, 448 (1991).